# Amorphization mechanisms in ion-bombarded metallic alloys

Abdenacer Benyagoub and Lionel Thomé
*Centre de Spectrométrie Nucléaire et de Spectrométrie de Masse, Bâtiment 108, 91405 Orsay, France*
(Received 28 December 1987)

A model of amorphous phase formation in ion-bombarded metallic alloys is proposed and compared to experimental results recorded with various techniques. The elementary mechanism is the formation of small amorphous clusters in the bombarded layer as soon as a favorable short-range order (threshold ion concentration) and a given topological disorder (threshold defect concentration) are locally established. The influence of the bombardment temperature is also discussed. Statistical considerations concerning the final spatial distributions of ions and defects allow us to account for the results obtained at low temperature, where implanted ions and radiation defects are immobile in the bombarded layer. A sigmoidal shape of the amorphization kinetics is obtained in implantation experiments or irradiation experiments with very light ions, while a nearly linear fluence dependence of the amorphous fraction is observed in irradiation experiments with heavy ions. At temperatures where implanted ions and radiation defects become mobile in the bombarded layer, the statistical description fails and ion trapping as well as defect recombinations have to be considered to reproduce experimental data. There is evidence that the amorphization model described in this paper for metallic systems also holds for other crystalline materials such as semiconductors or insulators.

## I. INTRODUCTION

The study of amorphous metallic alloys[1] is interesting from the double point of view of fundamental research (study of the influence of the structure on the physical properties of an alloy) and technological applications (for example, the possibility of improving the hardness and ductility of materials or reducing their corrosion). Among the large variety of techniques generally used to prepare metallic glasses (splat-cooling, vapor quenching, sputtering, electrodeposition, or chemical deposition), ion bombardment presents the advantage of allowing a direct study of the mechanisms by which amorphization occurs.

An energetic ion which penetrates into a solid loses its energy via both electronic excitation and/or ionization and elastic collisions with the nuclei of the target atoms before coming to rest in the host lattice. The latter process (nuclear energy loss), dominant at low ion velocity, leads to the creation of radiation damage. Amorphization of a crystalline metallic alloy by an ion beam then generally results from the presence of lattice disorder and impurities acting as disorder stabilizers. The temperature at which the system is bombarded is an important parameter for the study of the amorphization mechanisms since it governs the mobility of both implanted ions and defects.

Several models describing the amorphization of crystalline solids by ion bombardment have been developed[2–19] which stress the respective roles of radiation damage production and implanted species in the amorphization process. In the case (hereafter referred to as "irradiation" experiments) where the chemical short-range order (CSRO) of the amorphous system is basically identical to that of the ordered compound (semiconductors, metallic alloys presenting an amorphous counterpart), atomic displacements are only needed for amorphization. The amorphization mechanisms are then supposed[2–9,13–16,18] to depend mainly on the energy density deposited by the ion beam. In the displacement spike regime (irradiation with heavy ions), amorphization would result from a direct ion impact mechanism; in the linear cascade regime (irradiation with light ions), amorphization would be due to defect accumulation above a critical defect density. In the case (hereafter referred to as "implantation" experiments) where the CSRO of the system has to be modified in order to stabilize the induced amorphous structure, atomic displacements play no role in the amorphization kinetics since the topological disorder is already saturated at ion fluences far below the fluences generally involved. The amorphization models[10–12,17,19] are then more or less related to the compositional change of the implanted layer.

This paper attempts to unify the different approaches by the establishment of a unique model reproducing both irradiation and implantation experimental results. The foundations of this model are developed in Sec. II. Section III provides examples of application of the model to recent experimental results. The values of the different parameters extracted from the analysis of the amorphization kinetics are discussed in the last section.

## II. MODEL OF AMORPHIZATION BY ION BOMBARDMENT

A large number of results concerning implantation,[10–12,17,19–41] irradiation,[38,40–63] and ion-mixing[64–81] experiments show that the crystalline-to-amorphous transition in ion-bombarded metallic alloys generally results from the combination of two effects: disorder production (radiation damage) and stabilization of the disorder by the establishment of a favorable CSRO (already existing in the alloy or brought by implanted ions). Since the

 

fraction of amorphous volume (amorphous fraction) in ion-bombarded systems changes continuously with the ion fluence,[10,12,19,37,38,40,41,47,51–54,57,59–63] it is clear that this transition is not global but occurs locally. We are then led to the assumption that amorphization takes place by the formation of amorphous islands (called in the following amorphous clusters) as soon as the concentration of defects and stabilizer atoms locally exceed a given threshold concentration.

As far as the general case, where both implanted ions and defects play a role in the amorphization process, is considered, the calculation of the fluence dependence of the amorphous fraction (amorphization kinetics) must develop a functional relation between the spatial distributions of ions and defects. Such a relation is not easy to derive, due to the large number of parameters (nature of the incident ion and of the target, incident-ion energy, temperature, etc.) to be considered. Nevertheless, since the number of defects present in a small volume $v$ of the ion-bombarded crystal weakly depends on the number of ions implanted into this volume (radiation defects present in $v$ are generally issued from incident ions coming to rest outside of $v$), it is possible, in a first approximation, to assume that the concentrations of ions and defects located in $v$ are independent.

In light of the hypotheses discussed above, the amorphous fraction at a given depth in a crystal subjected to ion bombardment can be written

$$\alpha=\sum_{d\geq d_c} P(d,T)\sum_{c\geq c_c} Q(c,T)=f(d,d_c,T)g(c,c_c,T)\ , \tag{1}$$

where $P(d,T)$ and $Q(c,T)$ are the probabilities that there will be, at a temperature $T$, a concentration of defects $d$ and a concentration of implanted atoms $c$ inside an elementary volume of the target, respectively, and $d_c$ and $c_c$ are the corresponding threshold concentrations for amorphization.

The derivation of $f(d,d_c,T)$ and $g(c,c_c,T)$ then strongly depends on the temperature range considered.

### A. Low-temperature limit

The low-temperature limit concerns the case where both implanted ions and created defects are totally immobile in the host alloy. The probability laws governing their spatial distribution will be examined in the following subsections.

#### 1. Ions

Since implanted ions are supposed to be immobile in the host alloy and according to the fact that ion implantation is a uniform process all over the target area, the spatial ion distribution in the implanted layer obeys Poisson statistics. Noting $\bar{N}_i$ as the mean number of ions (corresponding to a mean concentration $c$) implanted into the elementary volume $v$, the probability distribution of $N_i$ around $\bar{N}_i$ can be written

$$Q(c,T<T_i)=\frac{(\bar{N}_i)^{N_i}}{N_i!}\exp(-\bar{N}_i)\ . \tag{2}$$

According to Eq. (1), $g(c,c_c,T)$ is then

$$g(c,c_c,T<T_i)=\sum_{N_i=N_{ic}}^{\infty}\frac{(\bar{N}_i)^{N_i}}{N_i!}\exp(-\bar{N}_i)\ , \tag{3}$$

where $N_{ic}$ is the critical number of ions above which $v$ is amorphous ($N_{ic}$ corresponds to the threshold concentration $c_c$ in this volume) and $T_i$ is the temperature at which implanted ions become mobile.

#### 2. Defects

The statistics governing the spatial distribution of radiation damage cannot be described by the simple equation (2), since point defects are created in a cascade mechanism, involving the primary ion and different types of secondary knocked atoms (with various energies). Actually, each (primary or secondary) atom with an energy higher than the displacement threshold energy of the target atoms creates, in small volumes along its trajectory, a number of point defects (depending on its energy) according to a Poissonian process. Since, around the maximum disorder depth (which constitutes the region of interest in ion-beam-induced amorphization studies), the mean number of defects created per length unit is nearly constant, the number of secondary atoms with a given energy is in a quasisteady state in a volume $v$ located in this region. The probability to get $n_d$ defects initiated by a single primary atom in $v$ is then

$$p(n_d)\simeq\sum\prod_{i=1}^{k}\frac{(\bar{\mu}_i)^{\mu_i}}{\mu_i!}\exp(-\bar{\mu}_i)\ , \tag{4}$$

where $\mu_i$ (and $\bar{\mu}_i$) are the number (and mean number) of defects created in $v$ by the primary ($i=1$) and the secondary ($i\neq 1$) atoms, and where the sum is over all the $\mu_i$ with the condition $\sum_{i=1}^{k}\mu_i=n_d$.

Equation (4) can also be written

$$p(n_d)=\frac{(\bar{n}_d)^{n_d}}{n_d!}\exp(-\bar{n}_d) \tag{5}$$

with $\bar{n}_d=\sum_{i=1}^{k}\bar{\mu}_i$ as the mean number of defects per primary atom created in $v$, according to the slowing-down theories.[82,83]

Since the number of ions responsible for the creation of radiation defects is distributed following Poisson statistics (as demonstrated in Sec. II A) with a mean value $\bar{n}_i$, the probability of getting a total number of $N_d$ defects in $v$ at a given ion fluence obeys the compound Poisson law:

$$P(d,T<T_d)=\sum_{n_i=0}^{\infty}\frac{(\bar{n}_i)^{n_i}}{n_i!}\exp(-\bar{n}_i)\frac{(n_i\bar{n}_d)^{N_d}}{N_d!}\times\exp(-n_i\bar{n}_d) \tag{6}$$

with a mean value $\bar{N}_d=\bar{n}_i\bar{n}_d$ (corresponding to the mean defect concentration $d$), a variance $\sigma^2=\bar{n}_d^2\bar{n}_i+\bar{n}_d\bar{n}_i$, and a characteristic function

$$M(t)=\exp[\bar{n}_i(\exp\{\bar{n}_d[\exp(it)-1]-1\})] . \quad (7)$$

Equations (1) and (6) then lead to

$$f(d,d_c,T<T_d)=\sum_{N_d=N_{dc}}^{\infty}\sum_{n_i=0}^{\infty}\frac{(\bar{n}_i)^{n_i}}{n_i!}\exp(-\bar{n}_i)\times\frac{(n_i\bar{n}_d)^{N_d}}{N_d!}\exp(-n_i\bar{n}_d) , \quad (8)$$

where $N_{dc}$ is the critical number of defects above which $v$ is amorphous ($N_{dc}$ corresponds to the threshold concentration $d_c$ in this volume) and $T_d$ is the temperature at which radiation defects become mobile.

In order to make the analysis of experimental data easier, Eq. (8) can be simplified depending on the value of the mean number of defects created in $v$ per incident ion.

*a.* $\bar{n}_d \ll 1$ *(very-light ion or electron irradiation).* When $\bar{n}_d \ll 1$, the characteristic function (7) becomes

$$M_P(t)=\exp(i\bar{n}_i\bar{n}_d t-1) . \quad (9)$$

Since Eq. (9) represents the characteristic function of a Poisson law with a mean value $\bar{n}_i\bar{n}_d$, Eq. (8) can be written

$$f_P(d,d_c,T<T_d)=\sum_{N_d=N_{dc}}^{\infty}\frac{(\bar{n}_i\bar{n}_d)^{N_d}}{N_d!}\exp(-\bar{n}_i\bar{n}_d) . \quad (10)$$

*b.* $\bar{n}_d > 1$ *(heavy-ion irradiation).* The function $P(d,T<T_d)$ can be decomposed in many subpeaks $n_i$, of total area $(\bar{n}_i^{n_i}/n_i!)\exp(-\bar{n}_i)$, distributed following the expression $[(n_i\bar{n}_d)^{N_d}/N_d!]\exp(-n_i\bar{n}_d)$ with a standard deviation $\sigma_i=(n_i\bar{n}_d)^{1/2}$. When $\bar{n}_d>1$ the ratio between $\sigma_i$ and the spacing $\bar{n}_d$ between the various subpeaks becomes small. The first subpeaks are then well separated, so that they can be approximated by delta functions. As in Eq. (8), the integration starts from $N_{dc}$, which generally lies in the region of the first subpeaks where the contribution of subpeaks with high $n_i$ is negligible, equation (6) can then be approximated by

$$P_G(N_d)=\frac{(\bar{n}_i)^{n_i}}{n_i!}\exp(-\bar{n}_i)\delta_{(N_d,n_i\bar{n}_d)} , \quad (11)$$

where $\delta$ is the Kronecker delta and the characteristic function corresponding to (11) is given by

$$M_G(t)=\exp\{\bar{n}_i[\exp(i\bar{n}_d t-1)]\} . \quad (12)$$

It is worth noting that $M(t)$ tends to $M_G(t)$ when $t$ becomes small. In such a case, the first moments of the distributions (6) and (11) are close to each other. According to Eq. (11), Eq. (8) can be approximated by the well-known Gibbons's equation:[4]

$$f_G(d,d_c,T<T_d)=\sum_{N_d=N_{dc}}^{\infty}\frac{(\bar{n}_i)^{n_i}}{n_i!}\exp(-\bar{n}_i)\delta_{(N_d,n_i\bar{n}_d)} . \quad (13)$$

The major part of the experimental data concerning metallic alloys irradiated with heavy ions can be analyzed using Eq. (13). However, in some cases, it is necessary to consider the effect of bombarding ions on the fraction of the crystal which has already been amorphized (i.e., the creation of free volume inside the amorphous regions) leading to an increase of the size of these regions. This extension[38] of Gibbons's description is presented in the Appendix.

### B. Influence of the temperature

When the temperature at which the crystal is bombarded is high enough to allow implanted ions and point defects to migrate into the host lattice, Eqs. (3) and (8) are no longer valid. The influence of the mobility of both species on the derivation of $f(d,d_c,T)$ and $g(c,c_c,T)$ is discussed in the following subsections.

#### 1. Ions

Migration affects the final spatial distribution of ions. A simple way to account for the observed effect is to assume that ions implanted into a volume $v_m$ (corresponding to $N_m$ atoms) can migrate to trap themselves into a small volume $v$ inside $v_m$. This volume $v$ becomes amorphous as soon as it reaches a size $v_c$ and contains a number of implanted ions equal to the threshold value $N_{mc}$ (corresponding to the amorphization concentration $c_c$ and to the amorphization density $D_c$). As ion implantation continues, $v$ grows to attain the size of $v_m$ leading to total amorphization of the implanted layer by coalescence of such amorphous volumes.

Since the number of ions $N_m$ implanted into $v_m$ obeys a Poisson law (see Sec. II A 1) with a mean value $\bar{N}_m$ (corresponding to the mean density $D_m$), $g(c,c_c,T)$ can be written,[84] in analogy with the low-temperature case

$$g(c,c_c,T>T_i)=\frac{D_m}{D_c}\sum_{N_m=N_{mc}}^{\infty}\frac{(\bar{N}_m)^{N_m}}{N_m!}\exp(-\bar{N}_m)=\frac{c}{1-c}\frac{1-c_c}{c_c}\sum_{N_m=N_{mc}}^{\infty}\frac{(\bar{N}_m)^{N_m}}{N_m!}\exp(-\bar{N}_m) \quad (14)$$

with $N_{mc}=v_cD_c$ and $\bar{N}_m=v_mD_m$.

The derivation of the amorphization kinetics in a temperature range where $T$ is close to $T_i$ is more difficult since it implies a good knowledge of the mechanisms by which ion migration occurs.

#### 2. Defects

When radiation damage is concerned, the main effect of the temperature is to affect $N_d$ and $\bar{n}_d$ (in a first approximation $N_{dc}$ can be considered as unaffected) since

defect recombinations, due to migration, occur. Equation (8) remains valid but $N_d$ and $\bar{n}_d$ must be replaced, respectively, by the number $N_{dr}$ and mean number $\bar{n}_{dr}$ of defects remaining in the volume $v$ after recombination. Approximations (10) and (13) are then no longer based on the value of $\bar{n}_d$ but on the value of $\bar{n}_{dr}$ (which is obviously smaller), so that the amorphization kinetics can present a shape different from that obtained at low temperature for the same irradiating ion. Moreover, in all cases, for a given ion-target system, the irradiation fluence needed to reach total amorphization (or any value of $\alpha$) is necessarily greater than at low temperature. The ratio between the fluences required for total amorphization in both cases gives an indication of the degree of defect recombination.

## III. APPLICATION OF THE MODEL TO EXPERIMENTAL RESULTS

The amorphization model developed in the previous section allows us to derive expressions of the amorphous fraction as a function of the ion fluence at various temperatures. Experimentally the amorphization kinetics can be studied by several techniques with different sensitivities:[85] transmission electron microscopy (TEM), grazing x-rays (XR), hyperfine interactions (HFI), electrical resistivity (ER), and Rutherford backscattering and channeling (RBS). All these techniques permit analysis of the very thin layers involved in ion-beam experiments (a few thousand angstroms) and are able to detect small amounts of amorphous (or crystalline) volume embedded in a crystalline (or amorphous) matrix. It must also be noted that the last two techniques (ER and RBS) need additional information, obtained via a complementary diffraction technique (TEM or XR), to establish the amorphous nature of the phase formed.

Since no experiments have yet been performed to study simultaneously the influence of both terms in Eq. (1), we will consider in the following subsections the two extreme cases where either $g(c,c_c,T)$, or $f(d,d_c,T)$ governs the amorphization process.

### A. Implantation experiments

In implantation experiments, the CSRO of the system is modified by implanted species which allow the stabilization of the ion-beam-induced disorder. Concurrent atomic displacements play no role in the amorphization kinetics since the topological disorder is saturated at ion fluences far below the fluences generally required (higher than $10^{16}$ atoms $cm^{-2}$) to modify the CSRO. The function $f(d,d_c,T)=1$ in Eq. (1) and the amorphous fraction can be written with Eqs. (3) or (14), depending on the temperature range considered.

#### *1. Low-temperature experiments*

Figures 1 and 2 present RBS results recorded at 90 K on, respectively, metal-metalloid[10,38,40] and metal-metal[37,41] systems. Figure 3 presents XR results recorded at 80 K on metal-metalloid systems.[12,19] It is quite clear that the different curves, which all present a sigmoidal shape (with a marked ion-concentration threshold), are well reproduced with Eq. (3). The values of the critical ion concentrations $c_c$ (corresponding to $N_{ic}$) and critical volumes $v_c$ (obtained from $\bar{N}_i$) of the amorphous clusters formed, extracted from the fits to experimental data using (3), as well as the values of the ion concentrations $c_T$ at which total amorphization of the bombarded layer is reached, are given in Table I for the various systems studied.

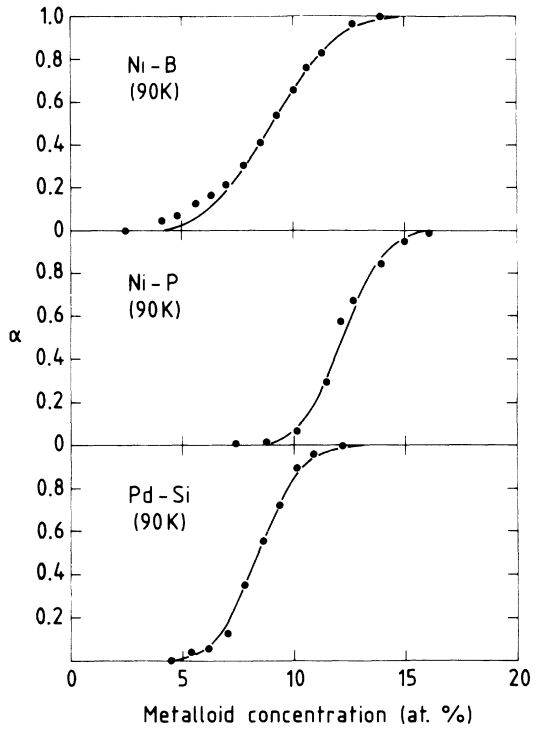


FIG. 1. Metalloid concentration dependence of the amorphous fraction $\alpha$ for 90-K-implanted metal-metalloid alloys, studied by RBS experiments. Solid lines represent the best fits to experimental data using Eq. (3) of the text.

#### *2. High-temperature experiments*

Experimental results recorded at room temperature, where implanted ions are mobile in the host lattice, are

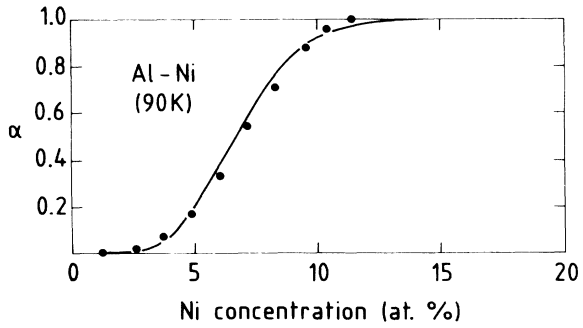


FIG. 2. Nickel concentration dependence of the amorphous fraction $\alpha$ for a 90-K-implanted Al-Ni alloy, studied by RBS experiments. The solid line represents the best fit to experimental data using Eq. (3) of the text.

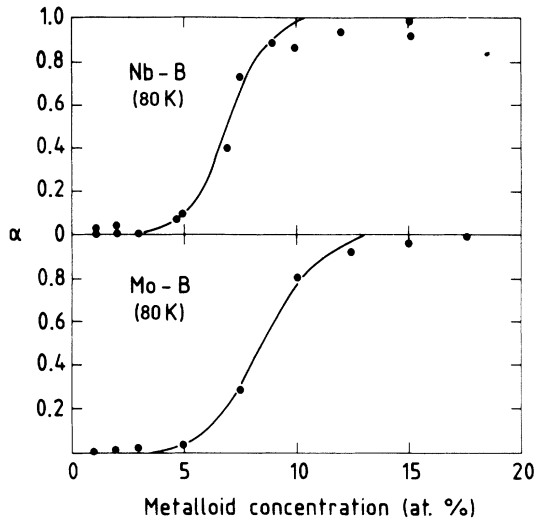


FIG. 3. Metalloid concentration dependence of the amorphous fraction $\alpha$ for 80-K-implanted metal-metalloid alloys, studied by XR. Solid lines represent the best fits to experimental data using Eq. (3) of the text.

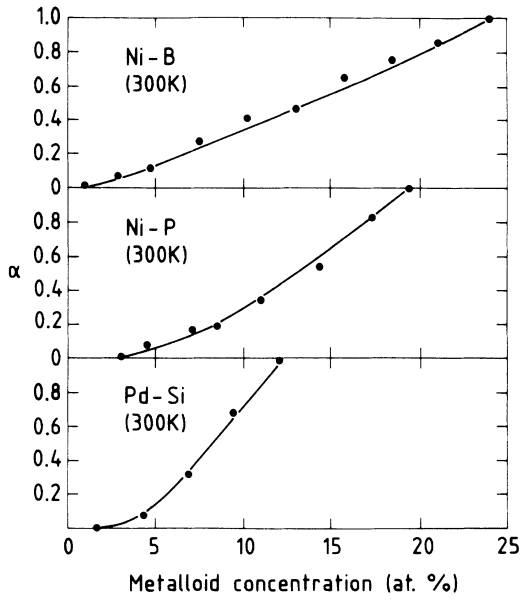


FIG. 4. Metalloid concentration dependence of the amorphous fraction $\alpha$ for 300-K-implanted metal-metalloid alloys, studied by RBS experiments. Solid lines represent the best fits to experimental data using Eq. (14) of the text.

are presented in Figs. 4 and 5 for, respectively, metal-metalloid[10,38] and metal-metal[37,41] systems studied by RBS, and in Fig. 6 for Nb-B studied by XR.[19] The different curves, which vary nearly linearly with the implanted ion concentration, are obviously well reproduced with Eq. (14). Table II gives the values of the critical ion concentrations $c_c$ and critical volumes $v_c$ of the amorphous clusters formed and of the migration volume $v_m$, extracted from the fits to experimental data using (14), as well as the values of the concentrations $c_T$ at which total amorphization occurs, for the various systems studied.

### B. Irradiation experiments

In irradiation experiments, the incoming ions create topological disorder without modifying the chemical nature of the alloy. This is achieved by implanting low fluences (generally less than $10^{15}$ atoms $cm^{-2}$) of chemically inert ions or by using high-energy ions which do not come to rest in the amorphized layer. In this case, as the alloy composition remains fixed (with $c > c_c$), $g(c,c_c,T)=1$ and the amorphous fraction can be written with the general equation (8) or with approximations (10) or (13) depending on the mass of the irradiating ion, i.e., on the value of $\bar{n}_d$.

The value of $\bar{n}_d$ can unfortunately not be *a priori* calculated for a given ion-target combination, since it depends on the volume $v_c$ of the amorphous clusters formed during irradiation. However, it is possible, from the slowing-down theories,[82,83] to calculate the mean number of defects created per length unit by an incoming ion: $d\bar{\nu}/dt$. The experimental results recorded in the case of implantation experiments have shown that the values of $v_c$ deduced for the various systems studied are very close to each other and lie between $1\times10^{-21}$ and $4\times10^{-21}$ $cm^3$ (see Table I), leading to a mean diameter (assuming spherical clusters) of the order of 10 Å. We will therefore in the following discuss the irradiation results via the parameter $d\bar{\nu}/dt$ where the depth interval $dt$ will be taken equal to 10 Å.

TABLE I. Parameters extracted from the fits to experimental data recorded on low-temperature ion-implanted metallic alloys using Eq. (3) of the text. $c_c$ and $v_c$ are, respectively, the critical ion concentration and critical volume of the amorphous clusters formed; $c_T$ is the ion concentration at which total amorphization is achieved.

| System | Implantation temperature (K) | $c_c$ | $v_c$ ($cm^3$) | $c_T$ | Ref. |
|---|---|---|---|---|---|
| Ni-P | 90 | 0.120 | $4.0\times10^{-21}$ | 0.150 | 10,38 |
| Ni-B | 90 | 0.093 | $1.5\times10^{-21}$ | 0.140 | 38,40 |
| Pd-Si | 90 | 0.085 | $4.0\times10^{-21}$ | 0.120 | 38 |
| Nb-B | 80 | 0.072 | $4.0\times10^{-21}$ | 0.140 | 12 |
| Mo-B | 80 | 0.085 | $4.0\times10^{-21}$ | 0.150 | 19 |
| Al-Ni | 90 | 0.070 | $2.0\times10^{-21}$ | 0.115 | 37,41 |

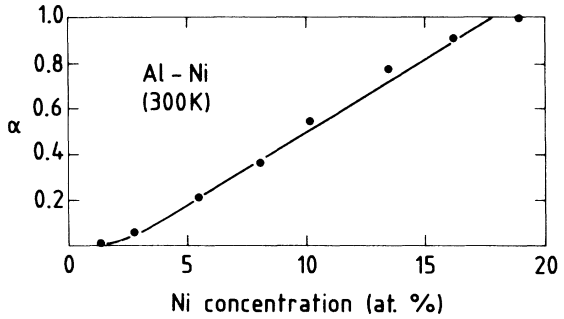


FIG. 5. Nickel concentration dependence of the amorphous fraction $\alpha$ for a 300-K-implanted Al-Ni alloy, studied by RBS experiments. The solid line represents the best fit to experimental data using Eq. (14) of the text.

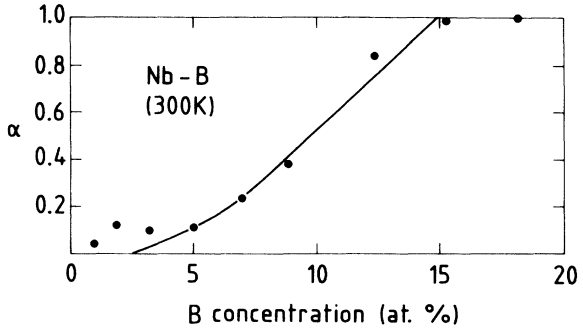


FIG. 6. Boron concentration dependence of the amorphous fraction $\alpha$ for a 300-K-implanted Nb-B alloy, studied by XR. The solid line represents the best fit to experimental data using Eq. (14) of the text.

### *1. Very-light-ion irradiation*

For the case of very-light-ion irradiation where $\bar{n}_d \sim d\bar{v}/dt \ll 1$ (H, He-ion, and electron irradiation), Eq. (8) reduces to Eq. (10). In this equation, $\bar{n}_i \bar{n}_d = v_c \Phi \, d\bar{v}/dt$, where $v_c$ is the critical volume of the amorphous clusters formed and $\Phi$ is the irradiation fluence.

Figure 7 presents RBS results recorded on the $Ni_3B$ (Refs. 41 and 62) and NiAl (Ref. 63) systems irradiated at 15 K with D ions. According to Eq. (10), the amorphization kinetics exhibits in both cases a sigmoidal shape with a clear ion-fluence threshold. The values of the critical defect concentrations $d_c$ (corresponding to $N_{dc}$) and critical volumes $v_c$ of the amorphous clusters formed, extracted from the fits to experimental data using (10), as well as the values of $d\bar{v}/dt$ and of the defect concentrations $d_T$ required to reach total amorphization of the irradiated layer, are given in Table III for the two systems studied.

### *2. Heavy-ion irradiation*

In the model developed in Sec. II, heavy-ion irradiation means irradiation with ions such that $\bar{n}_d \sim d\bar{v}/dt > 1$ (in most cases ions with a mass higher than that of boron). Equation (8) can then be approximated by Eq. (13), in which $\bar{n}_i = a\Phi$ where $a$ is the amorphization cross section, or leads to the extended Gibbons's equation (A10).

Figures 8 and 9 present RBS and ER results recorded, respectively, on the $Ni_3B$ (Refs. 38, 40, 54, and 61) and NiAl (Refs. 57 and 59) systems irradiated at various temperature with ions of mass ranging from B to Bi. The amorphization kinetics obviously depend on the value of $N_{dc}$ and are well reproduced using Eq. (13) or the modified equation (A10). The values of the critical defect concentrations $d_c$ and critical numbers of ion impacts $n_{ic}$ (both corresponding to $N_{dc}$) required to form an amorphous cluster, and of the parameters $a$ and $b$, extracted from the fits to experimental data using (13) or (A10), as well as the values of the defect concentrations $d_T$ at which total amorphization occurs, are given in Table IV for the systems represented in Figs. 8 and 9. This table also reports the values of these parameters obtained in the case of $Ni_3B$ (Refs. 38 and 61) and NiTi (Refs. 52 and 53) alloys irradiated at room temperature with various ions.

## IV. DISCUSSION

Tables I–III present the values of the critical ion ($c_c$) and defect ($d_c$) concentrations and of the critical volumes ($v_c$) of the amorphous clusters formed in ion-implanted and light ion-irradiated systems. It can be noticed that at low implantation temperature, $c_c$ varies from 0.07 (for Al-Ni) to 0.12 (for Ni-P), i.e., values well below those cor-

TABLE II. Parameters extracted from the fits to experimental data recorded on high-temperature ion-implanted metallic alloys using Eq. (14) of the text. $c_c$ and $v_c$ are, respectively, the critical ion concentration and critical volume of the amorphous clusters formed; $v_m$ is the volume inside which implanted ions can migrate to form amorphous clusters of volume $v_c$; $c_T$ is the ion concentration at which total amorphization occurs.

| System | Implantation temperature (K) | $c_c$ | $v_c$ (cm$^3$) | $v_m$ (cm$^3$) | $c_T$ | Ref. |
|---|---|---|---|---|---|---|
| Ni-P | 300 | 0.19 | $1.4\times10^{-22}$ | $3.0\times10^{-22}$ | 0.19 | 10,38 |
| Ni-B | 300 | 0.24 | $8.5\times10^{-23}$ | $1.0\times10^{-21}$ | 0.24 | 38 |
| Pd-Si | 300 | 0.12 | $4.3\times10^{-22}$ | $8.5\times10^{-22}$ | 0.12 | 38 |
| Pd-Si | 473 | 0.12 | $3.2\times10^{-22}$ | $1.2\times10^{-21}$ | 0.12 | 38 |
| Nb-B | 300 | 0.15 | $4.0\times10^{-22}$ | $1.0\times10^{-21}$ | 0.15 | 19 |
| Al-Ni | 300 | 0.18 | $2.3\times10^{-22}$ | $1.2\times10^{-21}$ | 0.18 | 37,41 |

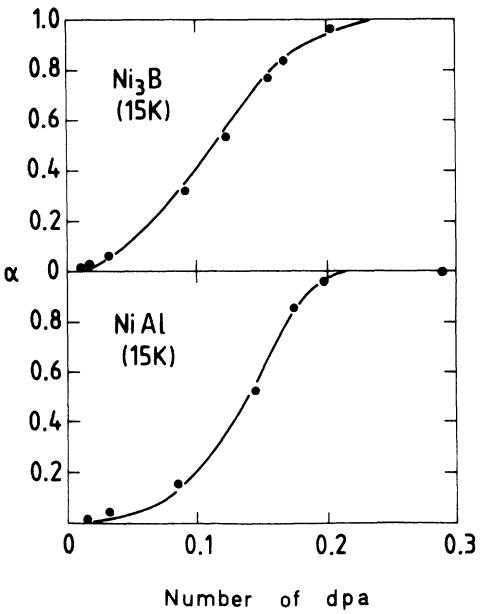


FIG. 7. Defect concentration dependence of the amorphous fraction $\alpha$ for $Ni_3B$ (upper curve) and NiAl (lower curve) alloys irradiated at 15 K with D ions, studied by RBS experiments. Solid lines represent the best fits to experimental data using Eq. (10) of the text. The irradiation fluence $\Phi$ has been converted into a number of displacements per atom (dpa) using the TRIM program (Ref. 83).

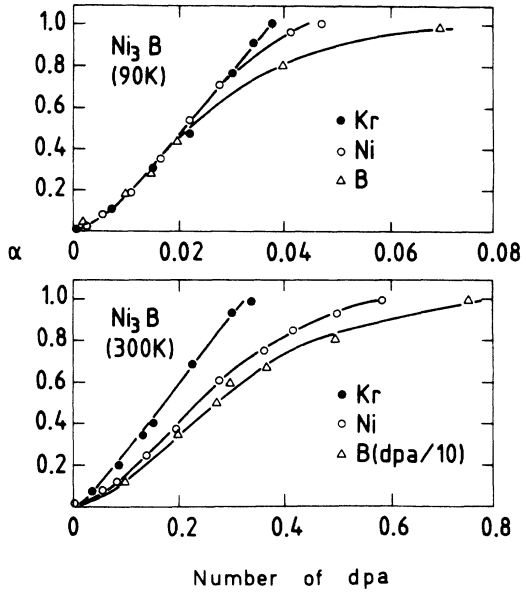


FIG. 8. Defect concentration dependence of the amorphous fraction $\alpha$ for a $Ni_3B$ alloy irradiated at 90 K (upper curve) and 300 K (lower curve) with ions of mass ranging from B to Kr, studied by RBS experiments. Solid lines represent the best fits to experimental data using Eq. (A10) of the Appendix. The irradiation fluence $\Phi$ has been converted into a number of dpa using the TRIM program (Ref. 83).

responding to eutectic or defined compound compositions in the alloy equilibrium phase diagram (at which systems prepared by quenching techniques become generally amorphous) but close to the bond-percolation threshold for the lattices considered. The values of $d_c$ found for the two alloys studied are also around 0.12. Values of $c_c$ very close to those reported in fast-quenching experiments are, however, obtained in the case of systems implanted at higher temperatures where ion migration was assumed to fit experimental data. The values of $v_c$, measured at temperatures where ions and defects are frozen in the host alloy, vary from $4.3\times10^{-22}$ cm$^3$ (radius $r_c=4.7$ Å assuming spherical clusters) for $Ni_3B$ irradiated with D ions to $4\times10^{-21}$ cm$^3$ ($r_c=9.8$ Å) for various implanted systems, i.e., the distance over which short-range order can be defined in a glassy material, and seem to depend on the nature and composition of the alloy rather than on the mass of the irradiating ion. A strong difference is here again noted with the results obtained at high implantation temperature where a reduction of the amorphous cluster size is evidenced ($r_c$ varying from 2.7 Å for B-implanted Ni to 4.7 Å for Si-implanted Pd).

A thermodynamical calculation[38] of the energy needed to form a spherical amorphous cluster of radius $r$ allows us to understand the origin of this temperature effect. The total work required to form such a cluster is the sum of the free volume enthalpy variation $\Delta G_v$, associated with the external energy $E_{\text{ext}}$ supplied to the system by ion bombardment, and of the free surface enthalpy variation $\Delta G_s$ due to the creation of the crystalline-amorphous interface. Calling $c$ the alloy composition and $T$ the temperature, this total work can be written

$$W(r,c,T)=(\tfrac{4}{3}\pi r^3)[G_a(c,T)-G_c(c,T)-E_{\text{ext}}] +4\pi r^2\sigma(c,T)\ , \tag{15}$$

TABLE III. Parameters extracted from the fits to experimental data recorded on metallic alloys irradiated with very light ions using Eq. (10) of the text. $d_c$ and $v_c$ are, respectively, the critical defect concentration and critical volume of the amorphous clusters formed; $d_T$ is the defect concentration at which total amorphization is achieved; $d\bar{\nu}/dt$ is the mean number of defects per incident ion created over a distance of 10 Å during irradiation, calculated using the TRIM program (Ref. 83).

| Target | Ion (energy) | Irradiation temperature (K) | $d_c$ | $v_c$ (cm$^3$) | $d_T$ | $d\bar{\nu}/dt$ | Ref. |
|---|---|---|---|---|---|---|---|
| $Ni_3B$ | D (15 keV) | 15 | 0.11 | $4.3\times10^{-22}$ | 0.22 | 0.08 | 41,62 |
| NiAl | D (15 keV) | 15 | 0.13 | $1.2\times10^{-21}$ | 0.21 | 0.12 | 63 |

where $G_c$ and $G_a$ are the free enthalpies per volume unit of the crystalline and amorphous phases, respectively, and $\sigma(c,T)$ is the surface free enthalpy of the crystalline-amorphous interface. The condition $(\partial W/\partial r)_{c,T}=0$ gives the critical radius of an amorphous cluster:

$$r_c(c,T)=\frac{2\sigma(c,T)}{E_{\text{ext}}-[G_a(c,T)-G_c(c,T)]} . \tag{16}$$

The temperature dependence of $G_c(c,T)$, $G_a(c,T)$, and $\sigma(c,T)$ must be established in order to account for the differences in the size of the critical volumes obtained in low- and high-temperature implantation experiments. As long as $T$ is lower than the glass transition temperature $T_g$, it is possible to write

$$\begin{aligned} G_c(c,T)&=H_c(c,T)-TS_c(c,T)\\ &=H_c(c,0)+\int_0^T \gamma_c(c,T')dT'\\ &\quad -T\int_0^T[\gamma_c(c,T')/T']dT' , \end{aligned} \tag{17a}$$

$$\begin{aligned} G_a(c,T)&=H_a(c,T)-TS_a(c,T)\\ &=H_a(c,0)+\int_0^T \gamma_a(c,T')dT'\\ &\quad -T\left[S_0+\int_0^T[\gamma_a(c,T')/T']dT'\right] , \end{aligned} \tag{17b}$$

where $H_c$ and $H_a$ are the formation enthalpies, $S_c$ and $S_a$ the entropies, $\gamma_c$ and $\gamma_a$ the specific heats of the crystalline and amorphous phases, respectively, and $S_0$ is the excess entropy of the amorphous phase. Assuming that, in a first approximation, $\sigma(c,T)$ is not affected by the in-

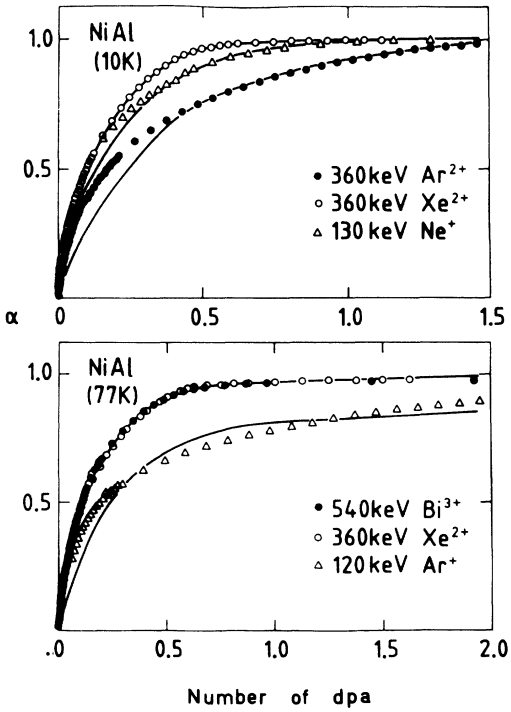


FIG. 9. Defect concentration dependence of the amorphous fraction $\alpha$ for a NiAl alloy irradiated at 10 K (upper curve) and 77 K (lower curve) with ions of mass ranging from Ne to Bi, studied by ER experiments. Solid lines represent the best fits to experimental data using Eq. (13) of the text. The irradiation fluence $\Phi$ has been converted into a number of dpa using the TRIM program (Ref. 83).

TABLE IV. Parameters extracted from the fits to experimental data recorded on metallic alloys irradiated with heavy ions using Eqs. (13) and (A10) of the text. $d_c$ and $n_{ic}$ are, respectively, the critical defect concentration and critical number of ion impacts required to amorphize a given region of the crystal; $a$ and $b$ are, respectively, the amorphization cross section and the expansion cross section of an amorphous cluster as it undergoes a subsequent ion impact; $d_T$ is the defect concentration at which total amorphization occurs; $d\bar{\nu}/dt$ is the mean number of defects per incident ion created over a distance of 10 Å during irradiation, calculated using the TRIM program (Ref. 83).

| Target | Ion (energy) | Irradiation temperature (K) | $d_c$ | $n_{ic}$ | $a$ (cm$^2$) | $b$ (cm$^2$) | $d_T$ | $d\nu/dt$ | Ref. |
|---|---|---|---|---|---|---|---|---|---|
| $Ni_3B$ | Kr (260 keV) | 90 | 0.030 | 2 | $2.4\times10^{-13}$ | $1.3\times10^{-13}$ | 0.038 | 38 | 38,54,61 |
| $Ni_3B$ | Ni (190 keV) | 90 | 0.027 | 2 | $2.0\times10^{-13}$ | $4.6\times10^{-14}$ | 0.048 | 28 | 38,54,61 |
| $Ni_3B$ | B (40 keV) | 90 | 0.026 | 2 | $1.5\times10^{-14}$ | | 0.070 | 2 | 38,54,61 |
| $Ni_3B$ | Kr (260 keV) | 300 | 0.22 | 2 | $3.3\times10^{-14}$ | $1.0\times10^{-14}$ | 0.34 | 38 | 38,61 |
| $Ni_3B$ | Ni (190 keV) | 300 | 0.28 | 2 | $1.9\times10^{-14}$ | $2.3\times10^{-15}$ | 0.58 | 28 | 38,61 |
| $Ni_3B$ | B (40 keV) | 300 | 5.4 | 2 | $7.0\times10^{-17}$ | | 7.5 | 2 | 38,61 |
| NiAl | Xe (360 keV) | 10 | 0.17 | 1 | $3.7\times10^{-14}$ | | 0.67 | 51 | 59 |
| NiAl | Ar (360 keV) | 10 | 0.36 | 1 | $3.0\times10^{-15}$ | | 1.0 | 9 | 59 |
| NiAl | Ni (130 keV) | 10 | 0.22 | 1 | $2.7\times10^{-15}$ | | 1.4 | 5 | 59 |
| NiAl | Bi (540 keV) | 77 | 0.18 | 1 | $5.3\times10^{-14}$ | | 0.65 | 80 | 57,59 |
| NiAl | Xe (360 keV) | 77 | 0.18 | 1 | $3.4\times10^{-14}$ | | 0.65 | 51 | 57,59 |
| NiAl | Ar (120 keV) | 77 | 0.25 | 1 | $7.7\times10^{-15}$ | | 3.5 | 16 | 57,59 |
| NiTi | Ni (390 keV) | 300 | 0.058 | 2 | $1.5\times10^{-13}$ | | 0.10 | 35 | 52 |
| NiTi | Ni (2.5 MeV) | 300 | 0.095 | 12 | $1.4\times10^{-13}$ | | 0.15 | 9 | 53 |
| NiTi | Ta (6 MeV) | 300 | 0.092 | 12 | $1.0\times10^{-12}$ | | 0.15 | 62 | 53 |

crease of the bombardment temperature and considering that, as experimentally demonstrated, $\gamma_a(c,T') \simeq \gamma_c(c,T')$ lead to the following expression of Eq. (16):

$$r_c(c,T) \simeq \frac{2\sigma(c)}{E_{\text{ext}} - [H_a(c,0) - H_c(c,0)] + TS_0} . \quad (18)$$

Equation (18) shows that, as experimentally observed, the critical radius of an amorphous cluster formed by ion bombardment grows as the temperature decreases. An estimation of the critical composition $c_c$ of amorphous clusters is in principle also possible using Eq. (15). Such a calculation, however, requires the knowledge of the variation of $\sigma(c,T)$ and $G_a(c,T)$ with $c$, quantities which have up to now been neither calculated nor experimentally measured.

The case of the irradiation of crystalline metallic alloys with heavy ions cannot, as indicated in the previous section, be described with Eqs. (3) or (10). It is thus not possible to make a full comparison between the parameters given in Table IV and Tables I–III. The defect concentration $d_c$ needed to amorphize a given volume of the bombarded layer has nevertheless been calculated in the different cases and appears to be lower for low-temperature heavy-ion-irradiated $Ni_3B$. If one excepts the case of Ne- and Ar-irradiated NiAl, for which the fits to experimental data are not very accurate (probably because of the problem of the analysis of the damage contribution at low fluence in ER experiments), it is worth noting that the amorphization cross section increases with the irradiating ion mass while $d_c$ is nearly independent of it. At room temperature, the number of ion impacts needed to amorphize a given region of the sample is generally the same as that at low temperature but the amorphization cross section is lower, certainly due to a high rate (higher in the case of light-ion irradiation) of defect recombinations. The case of the irradiation of NiTi with high-energy Ni and Ta ions is in this respect not clear. The large value of $n_{ic}$ needed to fit experimental results is a strong indication that the irradiation temperature was certainly higher than reported.

## V. CONCLUSION

In favorable cases, the mechanisms governing the crystalline-to-amorphous transition can be studied with ion bombardment since (contrary to the case of amorphization studies using classical quenching techniques) the amorphization process can be continually followed. The study, by various experimental methods, of the ion-fluence dependence of the amorphous fraction formed into the bombarded layer (amorphization kinetics) has shown that amorphization results from the creation (and coalescence) of amorphous islands (clusters) as soon as the concentration of both implanted ions (formation of a favorable CSRO) and created defects (topological disorder) locally exceeds a given threshold. The predominant role played by the ion-bombardment temperature has also been emphasized.

The elementary process occurs at a temperature where the implanted ions and radiation damage are totally immobile in the host alloy. The spatial distribution of these two species in the bombarded layer can then be calculated from statistical considerations alone.

The distribution of implanted ions obeys a simple Poisson law. In the case of implantation experiments, the amorphization kinetics then present a sigmoidal shape with a threshold ion concentration. Values of the critical ion concentrations $c_c$ and critical volumes $v_c$ of the amorphous clusters formed can be extracted from the fits to experimental data using this statistical representation. It is shown that $c_c$ varies very little with the alloy considered and is always small compared to the concentrations required in similar alloys prepared by fast-quenching techniques.

The distribution of radiation damage obeys a more sophisticated statistical law, due to the fact that defects are created in a cascade process. The general equation describing this process can be simplified in the two extreme cases where the number of defects created over a distance characteristic of the diameter of an amorphous cluster is either much smaller (very-light-ion irradiation) or greater (heavy-ion irradiation) than 1. In the former situation, the damage distribution can be reproduced using a simple Poisson law, so that the amorphization kinetics obtained for systems irradiated with H or He ions (and electrons) presents a sigmoidal shape (with a defect concentration threshold) as in the case of implantation experiments. The values of $v_c$ obtained from the fits are then close to the values of $v_c$ extracted from implantation data. The latter situation often leads to a linear fluence dependence (with an exponential saturation at high fluences) of the amorphous fraction, which can be ascribed to a direct ion impact amorphization mechanism. The fits to experimental data using an equation similar to that used by Gibbons in the case of semiconductor irradiation give values of the amorphization cross sections strongly dependent on the mass of the irradiating ion.

In the temperature range where implanted ions and radiation defects become mobile, additional hypotheses have to be used to account for experimental results. The nearly linear shape of the amorphization kinetics observed in implantation experiments can thus be reproduced by assuming that migrating ions trap themselves to form amorphous clusters at lower mean ion concentrations. Thermodynamical considerations show that the critical ion concentration required to form an amorphous cluster becomes comparable to that of a eutectic or a defined compound in the alloy equilibrium phase diagram and that the cluster size decreases. Irradiation experimental results have shown that bombardment with light ions (or electrons) generally does not lead to amorphous phase formation while bombardment with heavy ions may induce amorphization with a much smaller cross section, due to a significant rate of defect recombinations.

The amorphization mechanisms investigated in this paper concern ion-bombarded metallic alloys in an energy range where ions mainly lose their energy by nuclear elastic collisions with the target atoms. The amorphization model developed above can easily be extended to the case of other materials such as insulators or semiconductors. We must, however, stress that the ion-beam-induced amorphization experiments mentioned here to illustrate

the model are all limiting cases where either $f(d,d_c,T)$ or $g(c,c_c,T)$ is equal to 1. In order to definitely check the concomitance of CSRO modification and lattice disorder production [Eq. (1)] in the amorphization process, it would be particularly interesting to find a system where $f(d,d_c,T)$ and $g(c,c_c,T)$ vary separately and in a controlled way within the same experiment. It must finally be mentioned that a very different type of disordering process is presently observed at much higher ion energies (in the hundred MeV range) where electronic energy loss dominates the ion slowing-down process.[86–88]

## APPENDIX

This appendix presents an extension[38] of the model developed by Gibbons[4] in the case of ion irradiation of semiconductors. Here, we make the additional hypothesis that when an amorphous zone undergoes a subsequent ion impact, it expands, due to free volume creation, at the expense of the nearest, most disordered region[89] with a (mean) cross section $b$. This assumption leads to the coupled differential equation system:

$$\begin{aligned}
&\frac{dA_0}{d\Phi}=-aA_0\ ,\\
&\frac{dA_1}{d\Phi}=-aA_1+aA_0\ ,\\
&\vdots\\
&\frac{dA_k}{d\Phi}=-aA_k+aA_{k-1}\ ,\\
&\vdots\\
&\frac{dA_{n-1}}{d\Phi}=-aA_{n-1}+aA_{n-2}-b\alpha\ ,\\
&\frac{dA_n}{d\Phi}=\frac{d\alpha}{d\Phi}=b\alpha+aA_{n-1}\ ,
\end{aligned}\tag{A1}$$

where $A_k$ is the total normalized area of the region $k$ times disordered, $\Phi$ is the irradiation fluence, $a$ is the mean area disordered by a single ion impact, and $n$ is the number of ion impacts needed to amorphize $a$, with the following boundary conditions:

$$A_0+A_1+\cdots+A_k+\cdots+A_{n-1}+\alpha=1 \quad \text{for all } \Phi, \tag{A2}$$

$$A_0=1,\quad A_1=\cdots=A_k=\cdots=A_{n-1}=\alpha=0 \quad \text{for } \Phi=0\ . \tag{A3}$$

The solution of the first equation of system (A1) with the condition (A3) is

$$A_0=\exp(-a\Phi) \tag{A4}$$

while the other equations with $k\le n-2$, solved with the method of Green's function, give

$$A_k=\frac{(a\Phi)^k}{k!}\exp(-a\Phi)\ . \tag{A5}$$

In the case of Gibbons's model (where $b=0$), Eq. (A5) is valid for $k=n-1$ and the amorphous fraction is given by

$$\alpha=A_n=1-\sum_{k=0}^{n-1}A_k=1-\sum_{k=0}^{n-1}\frac{(a\Phi)^k}{k!}\exp(-a\Phi)\ . \tag{A6}$$

The solution of the last equation but one of the system (A1) is

$$A_{n-1}=\exp[-(a-b)\Phi]\int_0^{\Phi}\exp[(a-b)\Phi']d\Phi'\{aA_{n-2}(\Phi')-b+b[A_0(\Phi')+A_1(\Phi')+\cdots+A_{n-2}(\Phi')]\}$$
$$+C\exp[-(a-b)\Phi]\ , \tag{A7}$$

where $C$ is a constant.

After integration and consideration of the boundary conditions (A3), one obtains

$$A_{n-1}=\frac{b}{a-b}\left[1-\left[\frac{a}{b}\right]^n\exp[-(a-b)\Phi]\right]+\frac{(a\Phi)^{n-1}}{(n-1)!}\exp(-a\Phi)-\sum_{j=0}^{n-1}\left[\frac{a}{b}\right]^j\sum_{l=0}^{n-1-j}\frac{(a\Phi)^l}{l!}\exp(-a\Phi)\ . \tag{A8}$$

The amorphous fraction is then given by

$$\alpha=\frac{a}{a-b}\left[1-\left[\frac{a}{b}\right]^{n-1}\exp[-(a-b)\Phi]\right]-\sum_{l=0}^{n-1}\frac{(a\Phi)^l}{l!}\exp(-a\Phi)+\sum_{j=0}^{n-1}\left[\frac{a}{b}\right]^j\sum_{l=0}^{n-1-j}\frac{(a\Phi)^l}{l!}\exp(-a\Phi) \tag{A9}$$

which can also be written

$$\alpha=\frac{a}{a-b}\left[1-\left[\frac{a}{b}\right]^{n-1}\exp[-(a-b)\Phi]\right]+\sum_{j=1}^{n-1}\left[\frac{a}{b}\right]^j\sum_{l=0}^{n-1-j}\frac{(a\Phi)^l}{l!}\exp(-a\Phi)\ . \tag{A10}$$

It is worth noting that Eq. (A10) gives the well-known Gibbons's equation (A6) as $b$ tends to zero.

[1]See, for example, *Amorphous Metallic Alloys,* edited by F. E. Luborsky (Butterworths, London, 1983).
[2]J. R. Parson, Philos. Mag. **12**, 1159 (1965).
[3]F. F. Morehead and B. L. Crowder, Radiat. Eff. **6**, 27 (1970).
[4]J. F. Gibbons, Proc. IEEE **60**, 1062 (1972).
[5]H. M. Naguib and R. Kelly, Radiat. Eff. **25**, 1 (1975).
[6]J. R. Dennis and E. B. Hall, J. Appl. Phys. **49**, 1119 (1978).
[7]G. Carter and R. Webb, Radiat. Eff. Lett. **43**, 19 (1979).
[8]D. A. Thompson, Radiat. Eff. **56**, 105 (1981).
[9]V. V. Titov, Phys. Status Solidi A **63**, 11 (1981).
[10]C. Cohen, A. Benyagoub, H. Bernas, J. Chaumont, L. Thomé, M. Berti, and A. V. Drigo, Phys. Rev. B **31**, 5 (1985).
[11]V. Heera and B. Rauschenbach, Radiat. Eff. **91**, 71 (1985).
[12]G. Linker, Mater. Sci. Eng. **69**, 105 (1985).
[13]G. Carter, Radiat. Eff. **100**, 281 (1986).
[14]E. P. Simonen, Nucl. Instrum. Methods B **16**, 198 (1986).
[15]D. F. Pedraza and L. K. Mansur, Nucl. Instrum. Methods B **16**, 203 (1986).
[16]D. F. Pedraza, J. Mater. Res. **1**, 425 (1986).
[17]G. Linker, Solid State Commun. **57**, 773 (1986).
[18]D. F. Pedraza, Mater. Sci. Eng. **90**, 69 (1987).
[19]G. Linker, Nucl. Instrum. Methods B **19/20**, 526 (1987).
[20]P. V. Pavlov, E. I. Zorin, D. I. Tetelbaum, V. P. Lesnikov, G. M. Ryzhkov, and A. V. Pavlov, Phys. Status Solidi A **19**, 373 (1973).
[21]R. Andrew, W. A. Grant, P. J. Grundy, J. S. Williams, and L. T. Chadderton, Nature **262**, 380 (1976).
[22]A. G. Cullis, J. M. Poate, and J. A. Borders, Appl. Phys. Lett. **28**, 316 (1976).
[23]A. Ali, W. A. Grant, and P. J. Grundy, Philos. Mag. B **37**, 353 (1978).
[24]S. P. Singhal, H. Herman, and J. K. Hirvonen, Appl. Phys. Lett. **32**, 25 (1978).
[25]A. G. Cullis, J. A. Borders, J. K. Hirvonen, and J. M. Poate, Philos. Mag. B **37**, 615 (1978).
[26]W. A. Grant, Nucl. Instrum. Methods **182/183**, 809 (1981).
[27]G. Linker, Nucl. Instrum. Methods **182/183**, 501 (1981).
[28]B. Rauschenbach and K. Hohmuth, Phys. Status Solidi **172**, 667 (1982).
[29]C. Cohen, A. V. Drigo, H. Bernas, J. Chaumont, K. Królas, and L. Thomé, Phys. Rev. Lett. **48**, 1193 (1982).
[30]L. Mendoza-Zélis, L. Thomé, L. Brossard, J. Chaumont, K. Królas, and H. Bernas, Phys. Rev. B **26**, 1306 (1982).
[31]L. Thomé, A. Traverse, and H. Bernas, Phys. Rev. B **28**, 6523 (1983).
[32]J. D. Meyer and B. Stritzker, Z. Phys. B **54**, 25 (1983).
[33]G. Linker, Nucl. Instrum. Methods **209/210**, 969 (1983).
[34]L. Thomé, J. C. Pivin, A. Benyagoub, H. Bernas, and R. W. Cahn, Ann. Chim. Fr. **9**, 287 (1984).
[35]L. Thomé, A. Benyagoub, A. Audouard, and J. Chaumont, J. Phys. F **15**, 1129 (1985).
[36]A. Benyagoub, L. Thomé, A. Audouard, A. Chamberod, K. Królas, and P. Wodniecki, J. Non-Cryst. Solids **87**, 116 (1986).
[37]L. Thomé, F. Pons, J. C. Pivin, and C. Cohen, Nucl. Instrum. Methods B **15**, 269 (1986).
[38]A. Benyagoub, Ph.D. thesis, University of Orsay, 1986.
[39]W. Z. Li, Z. Al-Tamini, and W. A. Grant, Nucl. Instrum. Methods B **19/20**, 566 (1987).
[40]A. V. Drigo, M. Berti, A. Benyagoub, H. Bernas, J. C. Pivin, F. Pons, L. Thomé, and C. Cohen, Nucl. Instrum. Methods B **19/20**, 533 (1987).
[41]F. Pons, Ph.D. thesis, University of Orsay, 1987.
[42]L. M. Howe and M. H. Rainville, J. Nucl. Mater. **68**, 215 (1977).
[43]M. D. Rechtin, J. Van der Sande, and P. M. Baldo, Scr. Metall. **12**, 639 (1978).
[44]J. L. Brimhall, L. A. Charlot, and R. Wang, Scr. Metall. **13**, 217 (1979).
[45]J. D. Meyer and B. Stritzker, Z. Phys. B **36**, 47 (1979).
[46]A. E. Berkowitz, W. G. Johnston, A. Mogro-Campero, J. L. Walter, and H. Bakhru, in *Metastable Materials Formation by Ion Implantation,* Vol. 7 of *Materials Research Society Symposium Proceedings* (Elsevier, New York, 1982), p. 195.
[47]P. Moine, J. P. Rivière, N. Junqua, and J. Delafond, in *Metastable Materials Formation by Ion Implantation,* Ref. 46, p. 243.
[48]A. Wolthuis and B. Stritzker, J. Phys. (Paris) Colloq. **44**, C5-489 (1983).
[49]P. Moine, J. P. Eymery, R. J. Gaboriaud, and J. Delafond, Nucl. Instrum. Methods **209/210**, 267 (1983).
[50]J. L. Brimhall, H. E. Kissinger, and L. A. Charlot, Radiat. Eff. **77**, 237 (1983).
[51]C. Jaouen, J. P. Rivière, R. J. Gaboriaud, and J. Delafond, *Amorphous Metals and Nonequilibrium Processing* (Les Editions de Physique, Paris, 1984), p. 117.
[52]P. Moine, J. P. Rivière, M. O. Ruault, J. Chaumont, A. Pelton, and R. Sinclair, Nucl. Instrum. Methods B **7/8**, 20 (1985).
[53]J. L. Brimhall, H. E. Kissinger, and R. A. Pelton, Radiat. Eff. **80**, 241 (1985).
[54]A. Benyagoub, J. C. Pivin, F. Pons, and L. Thomé, Phys. Rev. B **34**, 4464 (1986).
[55]J. L. Brimhall and E. P. Simonen, Nucl. Instrum. Methods B **16**, 187 (1986).
[56]M. Nastasi, J. M. Williams, E. A. Kenik, and J. W. Mayer, Nucl. Instrum. Methods B **19/20**, 543 (1987).
[57]C. Jaouen, J. Delafond, and J. P. Rivière, J. Phys. F **17**, 335 (1987).
[58]D. Fournier, M. O. Ruault, and R. G. Saint-Jacques, Nucl. Instrum. Methods B **19/20**, 559 (1987).
[59]C. Jaouen, Ph.D. thesis, University of Poitiers, 1987.
[60]L. Thomé, J. Delafond, C. Jaouen, and J. P. Rivière, Nucl. Instrum. Methods B **19/20**, 554 (1987).
[61]L. Thomé, J. C. Pivin, F. Pons, and A. Benyagoub, Nucl. Instrum. Methods B **19/20**, 563 (1987).
[62]L. Thomé, F. Pons, E. Ligeon, J. Fontenille, and R. Danielou, J. Appl. Phys. **63**, 722 (1988).
[63]C. Jaouen, J. Delafond, J. P. Rivière, L. Thomé, F. Pons, R. Danielou, J. Fontenille, and E. Ligeon, J. Appl. Phys. (to be published).
[64]B. Y. Tsaur, S. S. Lau, L. S. Hung, and J. W. Mayer, Nucl. Instrum. Methods **182/183**, 67 (1981).
[65]G. Goltz, R. Fernandez, M. A. Nicolet, and D. J. K. Sadana, in *Metastable Materials Formation by Ion Implantation,* Ref. 46, p. 227.
[66]B. X. Liu, W. L. Johnson, M. A. Nicolet, and S. S. Lau, Nucl. Instrum. Methods **209/210**, 229 (1983).
[67]L. S. Hung, M. Nastasi, J. Gyulai, and J. W. Mayer, Appl. Phys. Lett. **42**, 672 (1983).
[68]B. Stritzker, *Amorphous Metals and Nonequilibrium Processing* (Les Editions de Physique, Paris, 1984), p. 141.
[69]J. Calliari, L. M. Gratton, L. Guzman, G. Principi, and C. Tosello, in *Ion Implantation and Ion Beam Processing of Materials,* Vol. 27 of *Materials Research Society Symposium Proceedings* (Elsevier, New York, 1984), p. 85.
[70]M. Van Rossum, V. Shreter, W. L. Johnson, and M. A. Nicolet, in *Ion Implantation and Ion Beam Processing of Materials,*

Ref. 69, p. 127.
[71]K. Saito and M. Iwaki, J. Appl. Phys. **55**, 4447 (1984).
[72]M. Van Rossum, M. A. Nicolet, and C. H. Wilts, J. Appl. Phys. **56**, 1032 (1984).
[73]R. S. Bhattacharya, A. K. Rai, and P. P. Pronko, Mater. Lett. **2**, 483 (1984).
[74]B. X. Liu, Nucl. Instrum. Methods B **7/8**, 547 (1985).
[75]C. Jaouen, J. P. Rivière, A. Bellara, and J. Delafond, Nucl. Instrum. Methods B **7/8**, 591 (1985).
[76]A. K. Rai, R. S. Bhattacharya, A. W. McCornik, P. P. Pronko, and M. Kholaib, Appl. Surf. Sci. **21**, 95 (1985).
[77]J. Bøttiger, N. J. Mikkelsen, S. K. Nielsen, G. Weyer, and K. Pampus, J. Non-Cryst. Solids **76**, 303 (1985).
[78]R. S. Averback, D. Peak, and J. L. Thompson, Appl. Phys. A **39**, 59 (1986).
[79]J. Eridon, L. Rehn, and G. Was, Nucl. Instrum. Methods B **19/20**, 626 (1987).
[80]J. Meissner, K. Kopitzki, G. Mertler, and E. Peiner, Nucl. Instrum. Methods B **19/20**, 669 (1987).
[81]B. X. Liu, E. Ma, J. Li, and L. J. Huang, Nucl. Instrum. Methods B **19/20**, 683 (1987).
[82]K. B. Winterbon, P. Sigmund, and J. B. Sanders, K. Dan. Vidensk. Selsk. Mat.-Fys. Medd. **37**, 14 (1970).
[83]J. P. Biersack and L. G. Haggmark, Nucl. Instrum. Methods **174**, 257 (1980).
[84]$D_c$ certainly depends on the size of the amorphous volume $v$ considered (Ref. 38). Here, we have (for the sake of simplicity) neglected this size dependence which has probably a minor effect (due to the fact that $v$ lies between $v_c$ and $v_m$ which are close to each other). To obtain the right-hand-side of Eq. (14), we have assumed that $D_c=[c_c/(1-c_c)]D$ and $D_m=[c/(1-c)]D$ where $D$ is the initial density of the bombarded crystal.
[85]L. Thomé, in *Nuclear Physics Applications on Materials Sciences,* Vol. 144 of *NATO Advanced Study Institute,* edited by E. Recknagel and J. C. Soares (Klumer, Norwell, MA, 1988), p. 183.
[86]S. Klaumünzer, M. D. Hou, and G. Schumacher, Phys. Rev. Let. **57**, 850 (1986).
[87]A. Audouard, E. Balanzat, G. Fuchs, J. C. Jousset, D. Lesueur, and L. Thomé, Europhys. Lett. **3**, 327 (1987).
[88]A. Audouard, E. Balanzat, G. Fuchs, J. C. Jousset, D. Lesueur, and L. Thomé, Europhys. Lett. **5**, 241 (1988).
[89]As a given amorphous zone is probably surrounded by a very disordered one and next by less and less damaged regions, it is reasonable to assume that, when an amorphous cluster is irradiated, it expands *only* at the expense of the most disordered zone. This hypothesis is all the more justified because this region is easier to amorphize. It must be emphasized that, if this assumption is not used, the expression of the amorphous fraction would contain too many extension parameters (each of them depending on the kind of zone in which this extension occurs).